Available online at www.sciencedirect.com

ScienceDirect

IFAC PapersOnLine 52-28 (2019) 164–169

Wide Range Stabilization of a Pendubot using quasi-LPV Predictive Control

Pablo S.G. Cisneros [*] **Herbert Werner** [*]

[*] *Hamburg University of Technology, Hamburg, Germany,*
(email: pablo.gonzalez@tuhh.de; h.werner@tuhh.de).

Abstract: This paper presents an experimental validation of a nonlinear predictive control law based on quasi-Linear Parameter Varying (q-LPV) modelling. q-LPV modelling is used to schedule the plant model, thereby turning the nonlinear optimization linear but time-varying, by imposing a scheduling sequence which is found iteratively. The pendubot is an interesting benchmark problem as the loci of equilibria lie on a nonlinear manifold; furthermore, the plant becomes increasingly hard to control the more the operating condition approaches one of the two uncontrollable equilibria. Unprecedented results are obtained using this control strategy by driving the system very close to said uncontrollable pose.

Keywords: Predictive control, linear parameter-varying, optimal control, inverted pendulum, pendubot

1. INTRODUCTION

The pendubot is an experimental platform often used in control education and research as a test bench for linear and nonlinear control strategies. As other inverted pendula it can be stabilized by linear control schemes in a small operating range. What sets it apart from other inverted pendula is that the loci of equilibria lie on a nonlinear manifold and nonlinear control strategies are therefore necessary if one is to stabilize the system on a wide operating region. Some examples of nonlinear control strategies that have been used for this benchmark problem are Olfati-Saber (2001), Spong and Block (1995) where nonlinear transformation (e.g. partial feedback linearization) is used to swing-up the pendulum; swing-up is also treated in Freidovich et al. (2008) using a method called virtual holonomic constraints. Finally, Kajiwara et al. (1998), Boonto (2011) use LPV gain-scheduling control techniques to stabilize the pendulum on a wide operating region.

In this paper we use qLMPC (or quasi-LPV MPC, Cisneros et al. (2016)) to control the pendubot and stabilize the origin from a perturbed initial condition. Furthermore the problem of wide operating region trajectory tracking is tackled as well. The qLMPC framework has been developed over some time and analytic results have been presented e.g. in Cisneros et al. (2016), Cisneros and Werner (2017), Cisneros and Werner (2018), experimental results have also followed in e.g. Cisneros et al. (2018). In this case, a new benchmark problem is presented in which it is shown that remarkable results are obtained by stabilizing the plant close to the uncontrollable positions while also displaying exceptional tracking performance. The paper is written in tutorial style, attempting to be thorough so that reproducibility can be readily achieved.

This paper is organized as follows: Section 2 introduces the plant and its model. Section 3 briefly reviews the qLMPC algorithm, while Section 4 discusses how stability is enforced within this framework, together with corresponding experimental results. Section 5 explores the tracking problem and the flexibility of the approach if one forgoes stability guarantees; experimental results are also presented. Finally, Section 6 concludes the paper.

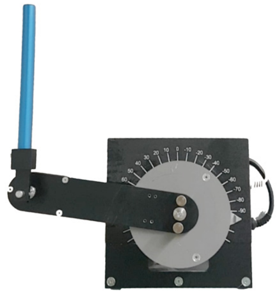

Fig. 1. Quanser planar rotary inverted pendulum

1.1 Notation

We denote a (block) diagonal matrix with elements $A, B, \ldots$ along the diagonal as $\text{diag}(A, B, \ldots)$. The *one vector* $[1\ 1\ \ldots\ 1]^\top$ of length N is denoted as $\mathbf{1}_N$. The Kronecker product of two matrices A and B is $A \otimes B$.

2. PLANT DESCRIPTION

The Pendubot, also known as Arm-Driven Inverted Pendulum (ADIP), is a planar 2-DOF robot which is actuated at the shoulder and unactuated at the elbow, see Figure 2. As opposed to other pendula often used as controller test benches, which only have two *distinct* equilibria (the stable ”down” and the unstable ”up”), the ADIP has a continuous locus of distinct (forced) equilibria, these can be categorized into

- DOWN-DOWN, $|\theta_1| > \pi/2$, $\theta_2 = \pi$

2405-8963 Δ 2019, IFAC (International Federation of Automatic Control) Hosting by Elsevier Ltd. All rights reserved.
Peer review under responsibility of International Federation of Automatic Control.
10.1016/j.ifacol.2019.12.367

- DOWN-UP $|\theta_1| > \pi/2$, $\theta_2 = 0$
- UP-DOWN $|\theta_1| < \pi/2$, $\theta_2 = \pi$
- UP-UP $|\theta_1| < \pi/2$, $\theta_2 = 0$

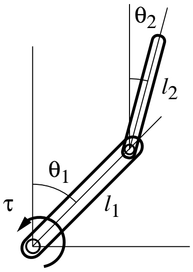

Fig. 2. Arm-driven inverted pendulum schematic

The goal throughout the paper is to stabilize the pendulum in its UP-UP configuration. The first proposed approach considers the regulator case, in which the objective is to stabilize the origin and bring the pendulum back from initial conditions within the domain of attraction to the origin. To this end, the stabilizing framework presented in Cisneros and Werner (2017) is to be used. In order to explore the full practical potential of the predictive control scheme, terminal constraints are later forgone and trajectory tracking is done aiming at wide operating conditions. Exactly why this is a particularly difficult task will become clear in what follows. The experiment is performed on a rotary inverted pendulum from Quanser (Figure 1), installed in planar configuration. The equations of motion are given by

$$M(\theta)\ddot{\theta} + C(\theta,\dot{\theta})\dot{\theta} + G(\theta) = \begin{bmatrix}\tau\\0\end{bmatrix} \tag{1}$$

where $\theta = [\theta_1 \quad \theta_2]^{\mathrm{T}}$,

$$M(\theta) = \begin{bmatrix}(m_1+m_2)l_1^2 & m_2l_1l_2\cos(\theta_1-\theta_2)\\ m_2l_1l_2\cos(\theta_1-\theta_2) & m_2l_2^2\end{bmatrix}$$

$$C(\theta,\dot{\theta}) = \begin{bmatrix}f_{v1} & m_2l_1l_2\sin(\theta_1-\theta_2)\dot{\theta_2}\\ -m_2l_1l_2\sin(\theta_1-\theta_2)\dot{\theta}_1 & f_{v2}\end{bmatrix}$$

$$G(\theta) = \begin{bmatrix}-(m_1l_{g1}+(m_h+m_2)l_1)g\sin(\theta_1)\\ -m_2l_2g\sin(\theta_2)\end{bmatrix}$$

and physical parameters are listed in Table 1.

2.1 quasi-LPV model

Given that the goal is to maintain $\theta_2 \approx 0$, a linearization can be carried out to simplify the model, furthermore using the substitution $\mathrm{sinc}(\theta) = \sin\theta/\theta$, the gravitational forces vector $G(\cdot)$ can be written as $G(\cdot) = K(\cdot)\theta$ yielding

$$\tilde{M}(\theta)\ddot{\theta} + \tilde{C}(\theta,\dot{\theta})\dot{\theta} + K(\theta)\theta = \begin{bmatrix}\tau\\0\end{bmatrix}$$

where

$$\tilde{M}(\theta) = \begin{bmatrix}(m_1+m_2)l_1^2 & m_2l_1l_2\cos(\theta_1)\\ m_2l_1l_2\cos(\theta_1) & m_2l_2^2\end{bmatrix}$$

$$\tilde{C}(\theta,\dot{\theta}) = \begin{bmatrix}f_{v1} & 0\\ -m_2l_1l_2\sin(\theta_1)\dot{\theta}_1 & f_{v2}\end{bmatrix}$$

$$K(\theta) = \begin{bmatrix}-(m_1l_{g1}+(m_h+m_2)l_1)g\,\mathrm{sinc}(\theta_1) & 0\\ 0 & -m_2l_2g\end{bmatrix}$$

which is readily turned into a qLPV model by defining the state to be $x = [\theta^{\mathrm{T}} \quad \dot{\theta}^{\mathrm{T}}]^{\mathrm{T}}$ and the scheduling parameter vector $\rho = [\theta_1 \quad \dot{\theta}_1]^{\mathrm{T}}$ leading to

Table 1. ADIP physical parameters

l_1	Arm length	13.95	cm
l_{g1}	Arm length (center of gravity)	6.975	cm
l_2	Pendulum length	7.8	cm
m_1	Arm mass	115	g
m_h	Encoder 2 mass	130	g
m_2	Pendulum mass	73.1	g
f_{v1}	Arm friction coefficient	$1.3 \cdot 10^{-3}$	N · s
f_{v2}	Pendulum friction coefficient	$2.2 \cdot 10^{-5}$	N · s

$$\begin{bmatrix}\dot{\theta}\\ \ddot{\theta}\end{bmatrix} = \underbrace{\begin{bmatrix}0 & I\\ -\tilde{M}(\rho)^{-1}K(\rho) & -\tilde{M}(\rho)^{-1}\tilde{C}(\rho)\end{bmatrix}}_{A_c(\rho)}\begin{bmatrix}\theta\\ \dot{\theta}\end{bmatrix} + \underbrace{\begin{bmatrix}0\\ \tilde{M}(\rho)^{-1}\end{bmatrix}}_{[B_c(\rho) \quad *]}\begin{bmatrix}\tau\\0\end{bmatrix}. \tag{2}$$

What makes the ADIP an interesting benchmark problem is that, not only do the loci of equilibria lie on a nonlinear manifold, the controllability of the system itself is strongly influenced by the pose of the arm to the point that it becomes uncontrollable if $\theta_1 = \pi/2$. This is illustrated in Figure 3 where the smallest singular value of the controllability Gramian of the pendubot at equillibrium positions in the range $-\pi/2 < \theta_1 < \pi/2$ is shown. The standard controllability Gramian is only defined for stable linear systems. In order to quantify the controllability of this system, the scheduling parameters are frozen at equilibrium points parameterized by θ_1. The Gramian for unstable linear system as proposed in Zhou et al. (1999) is used as an indicator of controllability of the resulting linear system. Intuitively, the plant becomes more difficult to control the more the operating condition approaches $\theta_1 = \pi/2$.

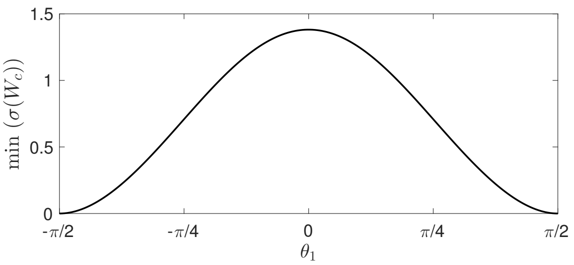

Fig. 3. Controllability Gramian at equilibrium positions for $-\pi/2 < \theta_1 < \pi/2$

3. QUASI-LPV MPC

The predictive control law is computed by minimizing a finite horizon objective function

$$J_k = \sum_{i=0}^{N-1} \ell(x_{k+i}, u_{k+i}) + \Psi(x_{k+N})$$

where the stage cost is defined as

$$\ell(x,u) = x^{\mathrm{T}}Qx + u^{\mathrm{T}}Ru \tag{3}$$

and the terminal cost function as $\Psi(x) = x^{\mathrm{T}}Px$. The optimization problem to be solved is thus

$$
\begin{aligned}
&\min_{\substack{u_k,\dots,u_{k+N-1}\\ x_{k+1},\dots,x_{k+N}}} J_k\\
&\text{s.t.}\\
&\quad x_{k+i+1} = A(\rho_{k+i})x_{k+i} + B(\rho_{k+i})u_{k+i}\\
&\quad u_{k+i} \in \mathcal{U} \qquad \forall i \in [0 \quad N-1]\\
&\quad x_{k+N} \in \mathbb{X}
\end{aligned}
\tag{P.1}
$$

where $\mathcal{U}$ is the set of admissible inputs and $\mathbb{X}$ is a terminal constraint set.

Quasi-LPV MPC (qLMPC) is an iterative algorithm which solves, at each time instant, a series of Quadratic Porgrams (QP) by freezing the scheduling trajectory

$$\mathsf{P}_k = \left[\rho_k^{\mathrm{T}}\ \rho_{k+1}^{\mathrm{T}}\ \dots\ \rho_{k+N-1}^{\mathrm{T}}\right]^{\mathrm{T}} \tag{4}$$

to the one given by the previous solution, essentially turning the quasi-LPV model (2) into a Linear Time-Varying (LTV) model at each iteration. Empirical evidence has shown that convergence is achieved typically in 1-2 iterations. Under these conditions, the equality constraint in problem (P.1) is linear and can be eliminated from the problem by substituting the future state trajectory into the cost function. The future state trajectory is given by

$$X_k = \Lambda(\mathsf{P}_k)x_k + S(\mathsf{P}_k)U_k \tag{5}$$

where

$$\Lambda(\mathsf{P}_k) = \begin{bmatrix} A(\rho_k)\\ A(\rho_{k+1})A(\rho_k)\\ \vdots\\ A(\rho_{k+N-1})A(\rho_{k+N-2})\dots A(\rho_k)\end{bmatrix},$$

$$S(\mathsf{P}_k) = \begin{bmatrix} B(\rho_k) & 0 & \dots\\ A(\rho_{k+1})B(\rho_k) & B(\rho_{k+1}) & \dots\\ \vdots & \vdots & \dots\\ A(\rho_{k+N-1})\dots B(\rho_k) & A(\rho_{k+N-1})\dots A(\rho_{k+2})B(\rho_{k+1}) & \dots \end{bmatrix}$$

and $U_k = [u_k^{\mathrm{T}}\ \dots\ u_{k+N-1}^{\mathrm{T}}]^{\mathrm{T}}$. The algorithm is summarized in Algorithm 1 [1].

Algorithm 1 qLMPC

```
Initialization:   plant model, $Q$, $R$, $N$
 1: $k \leftarrow 0$
 2: Define $\mathsf{P}^0 = \mathbf{1}_N \otimes f(x_k, u_{k-1})$
 3: repeat
 4:     $l \leftarrow 0$
 5:     repeat
 6:         Solve (P.1) using $\mathsf{P}_k^l$ to obtain $U_k^l$
 7:         Predict state $X_k^l = \Lambda(\mathsf{P}_k^l) + S(\mathsf{P}_k^l)U_k^l$
 8:         Define $\mathsf{P}_k^{l+1} = H(X^l, U^l)$
 9:         $l \leftarrow l + 1$
10:     until stop criterion
11:     Apply $u_k$ to the system
12:     Define $\mathsf{P}_{k+1}^0 = H(X_k^l, U_k^l)$
13:     $k \leftarrow k + 1$
14: until end
```

3.1 Observer design

An observer is used later in order to estimate disturbances, the chosen estimator is a quasi-LPV Kalman filter. This filter is similar to an Extended Kalman Filter (EKF), with the difference that the prediction for both the state and the covariance is done using the quasi-LPV model (2), as opposed to EKF where the state prediction is made using the nonlinear model (1) and the covariance prediction using the linearization of it. Nevertheless the structure is the same, the quasi-LPV estimation can be summarized as follows (based on EKF from Simon (2006)):

Predict:

$$
\begin{aligned}
\hat{x}_{k|k-1} &= A(\rho_{k-1})\hat{x}_{k-1|k-1} + B(\rho_{k-1})u_{k-1}\\
P_{k|k-1} &= A(\rho_{k-1})P_{k-1|k-1}A(\rho_{k-1}) + Q_e
\end{aligned}
$$

Update:

$$
\begin{aligned}
\tilde{y}_k &= y_k - C\hat{x}_{k|k-1}\\
K_k &= P_{k|k-1}C^{\mathrm{T}}(CP_{k|k-1}C^{\mathrm{T}} + R_e)^{-1}\\
\hat{x}_{k|k} &= \hat{x}_{k|k-1} + K_k\tilde{y}_k\\
P_{k|k} &= (I - K_kC)P_{k|k-1}
\end{aligned}
$$

where Q_e, R_e are the process and measurement noise covariances, often used as tuning parameters for estimation problems. Note that this observer uses a simple 1-step ahead prediction and the usual correction step (i.e. it is not a moving-horizon estimator).

4. STABILIZING QLMPC

Stability is established by the use of terminal ingredients and the *dual-mode* concept. In summary, the MPC law is used to drive the state into a terminal set within which a fictitious state feedback control law (the second-mode controller) generates admissible control inputs and renders the set positively invariant. This is formalized in the following Theorem (Cisneros and Werner (2017))

Theorem 1. (Stabilizing MPC for quasi-LPV systems). Assume a terminal controller $\tilde{F}(x_k, \rho_k) = F(\rho_k)x_k$, a terminal state domain $\mathbb{X}(\rho_k)$, a terminal cost function $\Psi(x_k, \rho_k)$ and an admissible parameter set $\mathcal{P}$ exist such that $\forall \rho \in \mathcal{P}$, $\forall k \in \mathbb{Z}^+$ the following conditions hold:

(1) $0 \in \mathbb{X}(\rho_k)$
(2) $(A(\rho_k) + B(\rho_k)F(\rho_k))x_k \in \mathbb{X}(\rho_k), \qquad \forall x_k \in \mathbb{X}(\rho_k)$
(3) $\Psi(0, \rho_k) = 0$, $\Psi(x_k, \rho_k) > 0 \quad \forall x_k \neq 0$
(4) $\Psi((A(\rho_k) + B(\rho_k)F(\rho_k))x_k, \rho_{k+1}) - \Psi(x_k, \rho_k) \leq -\ell(x_k, F(\rho_k)x_k), \quad \forall x_k \in \mathbb{X}(\rho_k)$
(5) $F(\rho_k)x_k \in \mathcal{U}, \qquad \forall x_k \in \mathbb{X}(\rho_k)$
(6) $\mathbb{X} \subset \mathrm{Im}(\varrho^{-1}(\mathcal{P}))$

Then, assuming feasibility of the initial state, an MPC controller solving the optimization problem (P.1) guarantees asymptotic stability of the origin and recursive feasibility.

In order to compute suitable terminal ingredients, the following result, which is a slight modification of the one presented in Cisneros and Werner (2017) [2] can be used. A

[1] In line 8, 12 of Algorithm 1, H maps the states and inputs to the parameters for the whole prediction horizon

[2] The modification consists in choosing the terminal set to be a sublevel set of the Lyapunov function, in order to derive convex conditions in the form of LMIs.

full derivation and proof of this version of the Theorem is given in Cisneros and Werner (2019).

Theorem 2. Let $Y(\rho) = P(\rho)^{-1}$, $X(\rho) = F(\rho)Y(\rho)$ and $\tilde{\alpha} = 1/\alpha$, then $\Psi(x, \rho) = x^{\mathrm{T}}P(\rho)x$, $\mathbb{X}(\rho) = \{x | x^{\mathrm{T}}P(\rho)x \leq \alpha\}$ and $F(\rho)$ satisfy the conditions of Theorem 1 if $Y(\rho)$ and $X(\rho)$ and $\tilde{\alpha}$ are chosen as the solutions to the optimization problem

$$\min_{X,Y,\tilde{\alpha},t} \; a_1\tilde{\alpha} + a_2 t \tag{6a}$$

s.t.

$$\begin{bmatrix} Y(\rho) & * & * & * \\ A(\rho)Y(\rho) + B(\rho)X(\rho) & Y(\rho + \Delta\rho) & * & * \\ Y(\rho) & 0 & Q^{-1} & * \\ X(\rho) & 0 & 0 & R^{-1} \end{bmatrix} \succeq 0, \tag{6b}$$

$$\begin{bmatrix} \tilde{\alpha}u^2_{i,max} & e_i X(\rho) \\ * & Y(\rho) \end{bmatrix} \succeq 0 \qquad i \in [1 \;\, m] \tag{6c}$$

$$e_j Y(\rho) e_j^{\mathrm{T}} \leq \tilde{\alpha}\overline{x}^2_{j,max} \qquad j \in [1 \;\, n_\rho] \tag{6d}$$

$$Y(\rho) \succ t \quad t > 0 \quad \tilde{\alpha} > 0 \qquad \forall \rho \in \mathcal{P},\; \Delta\rho \in \mathcal{V} \tag{6e}$$

In the above inequalities, $u_{max,i}$ denotes an upper bound on $|u_i|$, e_i is the i^{th} row of the identity matrix and $\overline{x}_j$ is the upper bound on parameter state x_j given by $\overline{x}_j = \max_{\mathcal{P}} |\varrho_l^{-1}(\rho_l)|, l = 1, ..., n_\rho$. The term $a_2 t$ in the objective function is added to improve the numerical conditioning of the Lyapunov matrix P as a_1, a_2 can be used as tuning parameters to penalize the largest eigenvalue of P.

The LMI problem in Theorem 2 is solved for a 4th order discretization of the quasi-LPV model in (2) with a sampling time of $T_s = 0.01$s. The discretization is obtained by a polynomial approximation of the matrix exponential leading to

$$A(\rho) = \frac{T_s^4}{24}A_c(\rho)^4 + \frac{T_s^3}{6}A_c(\rho)^3 + \frac{T_s^2}{2}A_c(\rho)^2 + T_s A_c(\rho) + I$$

$$B(\rho) = \frac{T_s^4}{24}A_c(\rho)^3 B_c(\rho) + \frac{T_s^3}{6}A_c(\rho)^3 B_c(\rho) + \frac{T_s^2}{2}A_c(\rho)B_c(\rho) + T_s B(\rho).$$

The tuning parameters are chosen as $Q = \mathrm{diag}(200, 1000, 0.1, 10)$, $R = 2000$, $N = 40$, and the admissible parameter set and parameter rate set, are chosen as

$$\mathcal{P} : \begin{cases} \rho_1 \in [-\pi/3 \;\;\, \pi/3] \\ \rho_2 \in [-1 \;\;\, 1] \end{cases} \qquad \mathcal{V} : \begin{cases} \Delta\rho_1 \in [-0.01 \;\;\, 0.01] \\ \Delta\rho_2 \in [-0.01 \;\;\, 0.01] \end{cases}$$

respectively. Note that admissible parameter values, and parameter rates are only specified for the second mode of the dual-mode controller, i.e. these sets do not limit the operating region as it is customary in LPV control; they can however limit the size of the terminal region given that by condition 6 in Theorem 1, the terminal region must be a subset of the of the inverse image of $\mathcal{P}$ on $\mathbb{R}^n$.

Both parameter dependent and independent terminal ingredients are obtained by solving the LMI problem (6), using the objective function $a_1\tilde{\alpha} + a_2 t$ where $a_1 = 0.5, a_2 = 10000$ for the parameter independent case and $a_1 = 5, a_2 = 10000$ for the parameter dependent case.[3] A comparison of the size of the resulting ellipsoids, projected onto planes of interest, is shown in Figure 4. In the figure, along with the ellipsoids, the projection of the admissible parameter values $\mathcal{P}$ onto the same planes is shown. In addition to admissible parameter values, both θ_2 and $\dot{\theta}_2$ are bounded as the equations of motions were linearized w.r.t these variables, so their values should not be large.

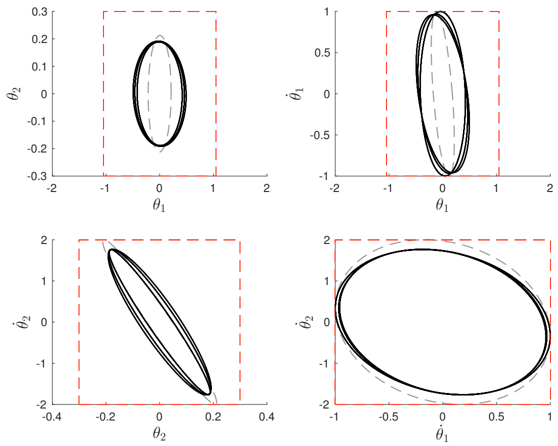

Fig. 4. Parameter independent (-----) and parameter dependent (——) ellipsoids, $\mathcal{P}_{\mathcal{X}}$ (-----)

4.1 Experimental result

The qLMPC algorithm is applied using both parameter dependent and independent terminal ingredients as discussed in the previous section. As the experimental setup uses incremental encoders (meaning the zero position is calibrated the moment the experiment is switched on) it is not possible to give arbitrary initial conditions for the regulator. To resolve this, the same MPC law, yet without terminal constraint is used to stabilize the system and drive it away from the origin (as disclosed in the following section) to give a non-zero initial condition to the MPC with terminal constraint and by extension stability guarantees, which is then enabled at $t = 20$s.

The closed-loop behavior in the experiments can be seen in Figure 5. Note that although the MPC with parameter independent terminal ingredients has better closed-loop performance, this is mainly due to the fact that the initial condition in the parameter dependent case is farther from the origin, as the comparatively larger ellipsoids enable a larger admissible set, if admittedly the difference is not excessive. In both cases performance is satisfactory and both stability and recursive feasibility are guaranteed by satisfaction of the terminal constraint at $k = 0$ (which corresponds to $t = 20$ s, i.e. when the MPC with stability guarantees is enabled). A graphical depiction of the terminal constraint is shown in Figure 6 in the $\theta_1 - \theta_2$-plane, where it is apparent that the predicted trajectory reaches the ellipsoid in both cases.

5. TRAJECTORY TRACKING - NO TERMINAL CONSTRAINTS

It is expected that stability guarantees come at a cost, in this case beside compromising feasibility on a wide operating region, redefining the terminal ingredients to apply

[3] The used weightings were empirically obtained to yield $\sigma_{\max}(P)$ in the same order for both cases.

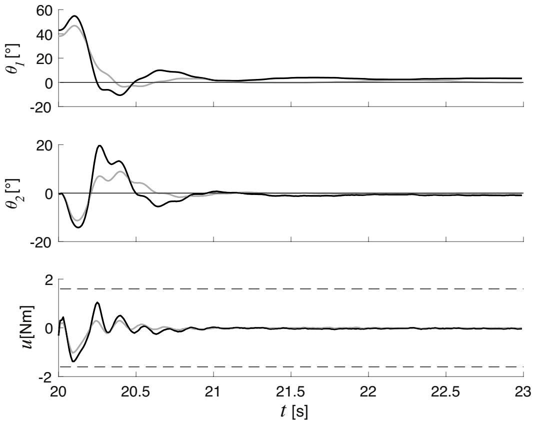

Fig. 5. Closed-loop response of MPC with parameter independent (——) and parameter dependent (——) terminal ingredients

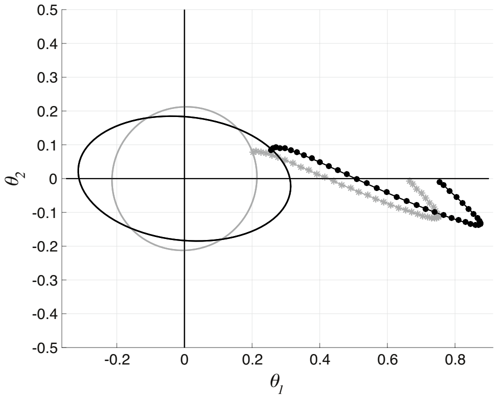

Fig. 6. Predicted trajectories of MPC with parameter independent (——) and parameter dependent (——) terminal ingredients at $k = 0$ and corresponding ellipsoids

to tracking is not practical as it would often necessitate a partition of the state space. If one relinquishes the terminal constraint, however, the algorithm becomes more flexible and outstanding tracking performance can be achieved. To explore this, this section tackles the problem of stabilizing the pendubot in as wide an operating region as possible. Consider the stage cost

$$\ell(x,u,x_s,u_s) = (x-x_s)^{\mathrm{T}}Q(x-x_s) + (u-u_s)^{\mathrm{T}}R(u-u_s) \tag{7}$$

where x_s is the desired steady state and u_s is the input corresponding to x_s. Assume initially that there is no disturbance, the steady state values are given by

$$x_s = [r \quad 0 \quad 0 \quad 0]^{\mathrm{T}}$$

and u_s is given by the solution to (note the absence of a disturbance)

$$\begin{bmatrix} I - A(\rho_s) & -B(\rho_s) \\ [1\ 0\ 0\ 0] & 0 \end{bmatrix} \begin{bmatrix} x_s \\ u_s \end{bmatrix} = \begin{bmatrix} 0 \\ r \end{bmatrix}.$$

Implementation of the control law as described above with tuning matrices $Q = \mathrm{diag}(700, 1000, 0.01, 10)$, $R = 2000$, $P = 1000Q$ and a prediction horizon of $N = 40$ results in the closed-loop response shown in Figure 7. While the range of operation is indeed remarkable, tracking performance, particularly in steady-state is not nearly as impressive. Clearly the assumption that the experiment is disturbance-free is unrealistic and modelling mismatches prevent adequate reference tracking.

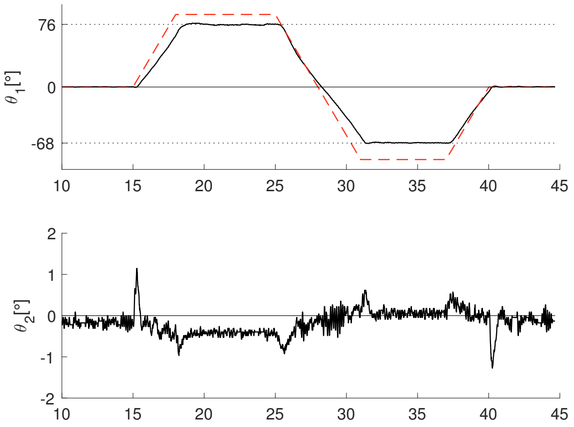

Fig. 7. Pendubot closed-loop response - no terminal constraint case

5.1 Disturbance models

A disturbance model can be included by augmenting the state with an integrating disturbance, i.e.

$$\begin{aligned} \begin{bmatrix} x_{k+1} \\ d_{k+1} \end{bmatrix} &= \begin{bmatrix} A(\rho_k) & B_d(\rho_k) \\ 0 & I \end{bmatrix} \begin{bmatrix} x_k \\ d_k \end{bmatrix} + \begin{bmatrix} B(\rho_k) \\ 0 \end{bmatrix} u_k + w_k \\ y_k &= [I \ \ C_d(\rho)] \begin{bmatrix} x_k \\ d_k \end{bmatrix} + v_k. \end{aligned} \tag{8}$$

where $B_d(\cdot)$, $C_d(\cdot)$ specify how the disturbance enters the state equation, and the output, respectively and w_k, v_k are zero-mean white noise processes driving these disturbances. The steady state input u_s is redefined to be the solution to

$$\begin{bmatrix} I - A(\rho_s) & -B(\rho_s) \\ [1\ 0\ 0\ 0] & 0 \end{bmatrix} \begin{bmatrix} x_s \\ u_s \end{bmatrix} = \begin{bmatrix} B_d(\rho_k)\hat{d} \\ r - C_d\hat{d} \end{bmatrix},$$

where $\hat{d}$ is the disturbance estimate. The steady state vector x_s, on the other hand, is not changed as in this case the reference always remains within the admissible region [4].

As a first approach it is assumed that the disturbance enters through the input, so that $B_d(\rho) = B(\rho)$, $C_d = 0$. An observer based on the augmented model (8) is used to estimate the disturbance with $Q_e = 100I_5$ and $R_e = 0.001I_2$. An MPC law using the augmented model (8), with tuning matrices $Q = \mathrm{diag}(1000, 1000, 0.1, 10, 0)$, $R = 2000$, $P = 1000Q$ considering the effect of input disturbances results in the closed-loop behavior shown in Figure 8. The addition of integral action through model augmentation together with the disturbance estimator yields vastly improved tracking performance, even though there is still steady-state error.

A close inspection of the time response plots leads to the conclusion that θ_2 is subject to an output disturbance given that the steady state value for $18 < t < 25$ is $\theta_2 \neq 0$

[4] This means that the reference is such that the corresponding steady state input is always admissible

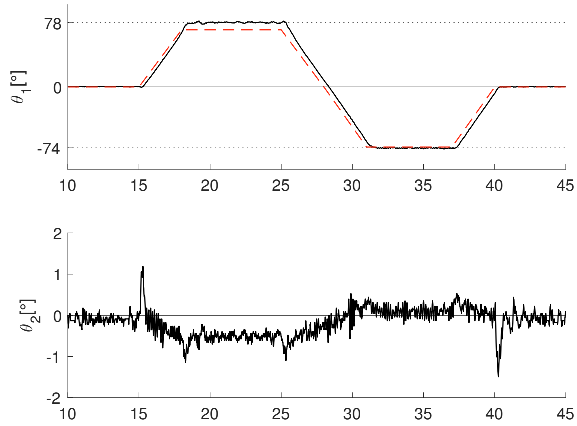

Fig. 8. Pendubot closed-loop response - no terminal constraint case using model augmented with disturbance

which is not physically possible. This disturbance is likely caused by an erroneous read of the sensor and it negatively impacts tracking performance. To capture this effect, a new disturbance model is included by defining

$$B_d(\rho) = [B(\rho) \;\; 0] \quad C_d = \begin{bmatrix} 0 & 0 \\ 0 & 1 \end{bmatrix}$$

which corresponds to a disturbance entering through the input and a disturbance directly acting on the output. As before, an observer is used for the augmented model in order to estimate the disturbances, the tuning parameters are $Q_e = 100I_6$ and $R_e = 0.001I_2$ and the MPC tuning matrices are set to $Q = \text{diag}(1000, 1000, 0.1, 10, 0, 0)$, $R = 2000$, $P = 1000Q$. The closed-loop response using this controller is shown in Figure 9, where it can be seen that the steady state error is not present anymore and satisfactory results are achieved. It is worth mentioning that compared to other approaches a remarkable range of $\theta_1 \in [-80° \;\; 80°]$ is achieved, whereas previous reported results achieved only ±65° Kajiwara et al. (1998), ±70° Boonto (2011)[5].

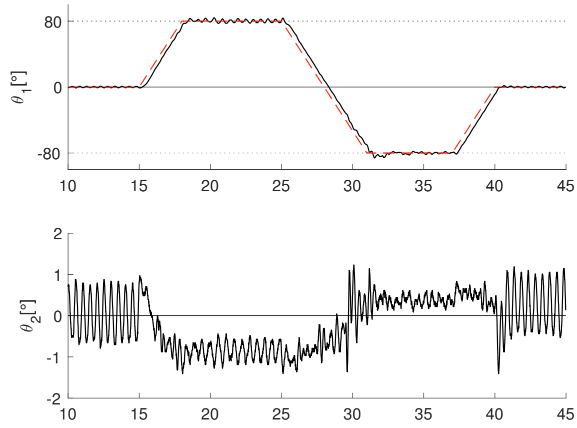

Fig. 9. Pendubot closed-loop response - no terminal constraint case using model augmented with 2 disturbances

6. CONCLUSIONS

The Pendubot benchmark problem is used to highlight the flexibility and capabilities of the qLMPC algorithm. The algorithm can be used in its stabilizing variant to obtain a guaranteed stable closed-loop by solving an LMI problem offline to determine the terminal ingredients and adding a terminal constraint. Forgoing this terminal constraint, however, makes the algorithm more flexible and trajectory tracking problems can be easily handled. Modelling errors and disturbances can be handled by state augmentation in a straightforward fashion. Nevertheless, the choice the disturbance model is seen to play an important role in the resulting closed-loop performance; relatively simple disturbance models are shown to yield satisfactory result.

REFERENCES

Boonto, S. (2011). *Identification of Linear Parameter-Varying Input-Output Models.* Ph.D. thesis, Hamburg University of Technology.

Cisneros, P.S.G., Voss, S., and Werner, H. (2016). Efficient nonlinear model predictive control via quasi-lpv representation. *55th IEEE Conference in Decision and Control.*

Cisneros, P.S.G. and Werner, H. (2017). Parameter dependent stability conditions for quasi-lpv model predictive control. *American Control Conference.*

Cisneros, P.S., Sridharan, A., and Werner, H. (2018). Constrained predictive control of a robotic manipulator using quasi-lpv representations. *IFAC-PapersOnLine*, 51(26), 118 – 123.

Cisneros, P.S. and Werner, H. (2018). A dissipativity formulation for stability analysis of nonlinear and parameter dependent mpc. In *2018 American Control Conference (ACC)*, 3894–3899. IEEE.

Cisneros, P.S. and Werner, H. (2019). Nonlinear model predictive control for models in quasi-lpv form. *submitted to International Journal of Robust and Nonlinear Control.*

Freidovich, L., Robertsson, A., Shiriaev, A., and Johansson, R. (2008). Periodic motions of the pendubot via virtual holonomic constraints: Theory and experiments. *Automatica*, 44(3), 785 – 791.

Kajiwara, H., Apkarian, P., and Gahinet, P. (1998). Wide-range stabilization of an arm-driven inverted pendulum using linear parameter-varying techniques. In *Guidance, Navigation, and Control Conference and Exhibit*, 4503.

Olfati-Saber, R. (2001). *Nonlinear control of underactuated mechanical systems with application to robotics and aerospace vehicles.* Ph.D. thesis, Massachusetts Institute of Technology.

Simon, D. (2006). *Optimal State Estimation.* John Wiley & Sons.

Spong, M.W. and Block, D.J. (1995). The pendubot: a mechatronic system for control research and education. In *Proceedings of 1995 34th IEEE Conference on Decision and Control*, volume 1, 555–556 vol.1.

Zhou, K., Salomon, G., and Wu, E. (1999). Balanced realization and model reduction for unstable systems. *International Journal of Robust and Nonlinear Control: IFAC-Affiliated Journal*, 9(3), 183–198.

[5] The latter result is obtained on the same physical platform